Journal of Metals, Materials and Minerals, 35(2), e2213, 2025

Investigation of pressure and temperature distributions in aerofoils using CFD simulation

Ramesh KRISHNAN L[1], Jasgurpreet Singh CHOHAN[2,3], S. VIJAYAKUMAR[4,5,*], N. BEEMKUMAR[6], Sriram DESIKAN[7], V. Nagabhushana RAO[8], M. Naga Swapna SRI[9], and Mayank KUNDLAS[10]

[1] *Department of Mechanical Engineering, KCG College of Technology, Karapakkam, Chennai-97*
[2] *University School of Mechanical Engineering, Rayat Bahra University, Kharar, Punjab 140103, India*
[3] *Faculty of Engineering, Sohar University, PO Box 44, Sohar, PCI 311, Oman*
[4] *Department of Mechanical Engineering, Graphic Era Hill University, Dehradun-248002, Uttarakhand, India*
[5] *Department of Mechanical Engineering, Graphic Era Deemed to be University, Dehradun-248002, Uttarakhand, India*
[6] *Department of Mechanical Engineering, School of Engineering and Technology, JAIN (Deemed to be University), Bangalore, Karnataka, India*
[7] *Department of Mechanical Engineering, Indra Ganesan College of Engineering, Trichy, Tamil Nadu*
[8] *Department of Mechanical Engineering,Raghu Engineering College, Visakhapatnam, Andhra Pradesh-531162, India*
[9] *Department of Mechanical Engineering,P V P Siddhartha Institute of Technology, Vijayawada*
[10] *Centre for Research Impact & Outcome, Chitkara University Institute of Engineering and Technology, Chitkara University, Rajpura, 140401, Punjab, India*

***Corresponding author e-mail**: vijaysundarbe@gmail.com

Received date:
25 November 2024
Revised date:
4 February 2025
Accepted date:
4 April 2025

Keywords:
Aerofoil;
M13;
Eppler 1233;
Computational;
Pressure co efficient

Abstract

Most aircraft derive the design of their wings, fins, and horizontal stabilizers from this construction approach, incorporating curved surfaces to enhance the lift-to-drag ratio during flight. Over the past decade, Computational Fluid Dynamics (CFD) has become the leading tool for designing components and processes involving fluid or gas movement across industries such as aviation, automotive, and manufacturing. This study examines the aerodynamic characteristics—including pressure, density, and temperature distribution, as well as lift and drag forces—of two different angles of attack based on the M13 and Eppler 1233 airfoils. The analysis considers an airfoil with varying chord thickness while maintaining a consistent maximum thickness as a percentage of the chord length. The primary objective of this research is to conduct a comprehensive numerical assessment of airfoil structures. A 2D computational simulation is performed on different airfoil shapes at angles of attack of 0° and 8° using ANSYS Fluent. The results reveal variations in flow characteristics across different structures and evaluate the balance between lift and drag forces at various angles of attack to enhance aerodynamic efficiency. According to the study, aerodynamic performance and stability are both enhanced when aerofoil designs are optimised to reduce turbulence and flow separation. This exemplifies the compromise that must be made to maximise aerodynamic performance by either increasing lift or controlling drag. The findings contribute to a deeper understanding of airflow over airfoil structures and its impact on aircraft performance.

1. Introduction

The fundamental structure of the wings, fins, and horizontal stabilizers of the majority of aircraft is based on this particular construction method, which utilizes curved surfaces to optimize the lift-to-drag ratio during flight. In order to adequately consider the substantial influence of wind, the utilization of a specialized aerofoil is imperative. A distinctive type of aerofoil was developed and introduced by the National Advisory Committee for Aeronautics (NACA) between the 1960s and 1970s. The front edge of this aerofoil is enlarged curved, while the top surface is flat, the trailing edge is straight, it has a supercritical shape, and the rear portion is curved. It is advisable to employ computational fluid dynamics (CFD) software in order to improve and streamline these models [1]. The primary objective of the aerofoil design is to reduce drag and mitigate the impact of shock waves. There is considerable interest from commercial aircraft manufacturers in producing the prototype once it is complete. This serves as a motivation for NASA to develop a diverse array of model iterations [2].

Various techniques may be used to modify the lift generated by an aircraft's wing. Lift augmentation devices are designed with the particular purpose of enhancing lift by altering the curvature of the wing, which is referred to as the camber. Numerous analogous devices have been developed, evaluated, and put into use. It is mostly used by aircraft to modify the wing's surface. Aerodynamic devices like as flaps, slots, and slats, either alone or in combination, have been used on almost all types of aircraft. Over the course of history, scientists have strived to develop aerofoils using various camber techniques, allowing the pilot to quickly adjust the characteristics of the aerofoil, ranging from increased lift to altered cruising speed. An elevating body is any object that generates upward forces, independent of its state of motion or rest. When developing these lifting appendages,

issues such as dimensions and configuration are meticulously taken into account. An aerofoil is a kind of movable structure. The lift to drag relationship determines the shape of this aerofoil. When this structure generates a substantial amount of upward force while encountering little resistance, it may be described as an efficient body. The experiment was carried out at a Reynolds number of 2.4105 utilizing a wind tunnel equipped with a six-component internal interface. Throughout the computer-aided design (CAD) process, several novel products were generated, all of which had the same plan shape and camber distribution as the NACA0010, NACA2410, and NACA8410 aerofoil sections [3-5]. The wings generated by scanning were then compared to additional test parts, which served as reference points for comparison. The results revealed that the test articles, which were produced via scanning and had constant camber distributions of 2% and 8%, exhibited comparable aerodynamic characteristics to the baseline wings that included the standardized NACA 2410 and 8410 aerofoil sections, respectively.

A singular actuator mechanism may govern the leading and trailing edges of the wing, and it is possible to detect the precise vertical displacement of each edge in reference to the spar. Optical measuring devices are used to evaluate alterations in wing structure, while XFLR software enables further analysis of 13 specific sections within the aerofoil. The analysis of the surface pressure coefficient reveals that the angle of attack (AOA) increases considerably between –4°C and 8°C, according to the test results. The metric is a quantitative measure employed to assess the extent of variability in maximal camber.

Static aero elasticity investigates the relationship between elastic and aerodynamic forces, whereas dynamic aero elasticity explores the interplay among inertia, elastic, and aerodynamic forces, in addition to control laws [7]. Aero-servo-elasticity refers to the study of the interaction between aerodynamics, structural dynamics, and control systems in aerospace engineering. Aero elastic research is crucial in the aircraft design and testing process because to the great flexibility of modern aircraft structures [12,13]. Wing tensional divergence and flutter are the two main aero elastic phenomena that are taken into account in aircraft design. Divergence is the result of the static aerodynamic forces exceeding the structural stiffness, causing instability. Flutter is a dynamic instability of a structure that occurs when the elastic, inertial, and aerodynamic forces acting on it combine, leading to prolonged oscillation. A method for improving the design of Turbine Aerofoils was developed utilizing Quasi-3D analytic techniques. By assembling several 2D aerofoil components in a spiral pattern utilizing smooth second and first order polynomials, without any sudden shifts in the radial direction [6].

The SolidWorks extruded model is imported into the analysis application, where several Computational Fluid Dynamics (CFD) simulations may be conducted [22-24]. The ANSYS software creates a bounding box around the NACA aerofoil and identifies its inlet, outlet, boundary, and blade profile. The analysis takes into account boundary conditions, such as a fixed angle of attack, constant air density, and velocity [11-13]. The objective of this study is to examine the aerodynamic properties of the different aerofoil shapes: The M13, and Eppler 1233. The emphasis is placed on quantifying the coefficients of lift and drag. An aerofoil having changes in the chord thickness at different points, but without changing the maximum thickness as a percentage of the chord. Here is a sequential strategy to achieve the ultimate objective. The aim of this work is to conduct a comprehensive investigation of the numerical aspects related to various aerofoil structures.

To create the computational model of the aerofoil designs.

Employ ANSYS-Fluent to analyse the unique flow characteristics across M13 and Eppler 1233 aerofoil designs.

The pressure, temperature and density distribution is explored at M13, and Eppler 1233 aerofoil structures

To analyse the balance between lift and drag forces at different angles of attack (0° and 8°) to enhance the aerodynamic characteristics.

2. Material and methods

The construction of a three-dimensional representation of an aerofoil and its associated framework is accomplished via CAD software [21,25]. Utilize computer-aided design (CAD) software, such as the design modeler, to produce an initial two-dimensional representation of the airfoil and its numerous components. This assignment requires the development of models for two distinct aerofoil configurations: the M13 and Eppler 1233. The approximate length of the airfoil is one meter. Utilizing the design modeler application, the two-dimensional structure is simulated. Adhering to conventional design principles, the aerofoil profile has a maximal width of approximately 0.75 m. Figure 1 displays two various airfoil shapes with different angles of attack.

The study will be performed with the geometric parameters recommended by the National Aeronautics and Space Administration. The simulation determines the distribution of pressure, velocity, and temperature by modifying the angle of attack of the 2D wings.

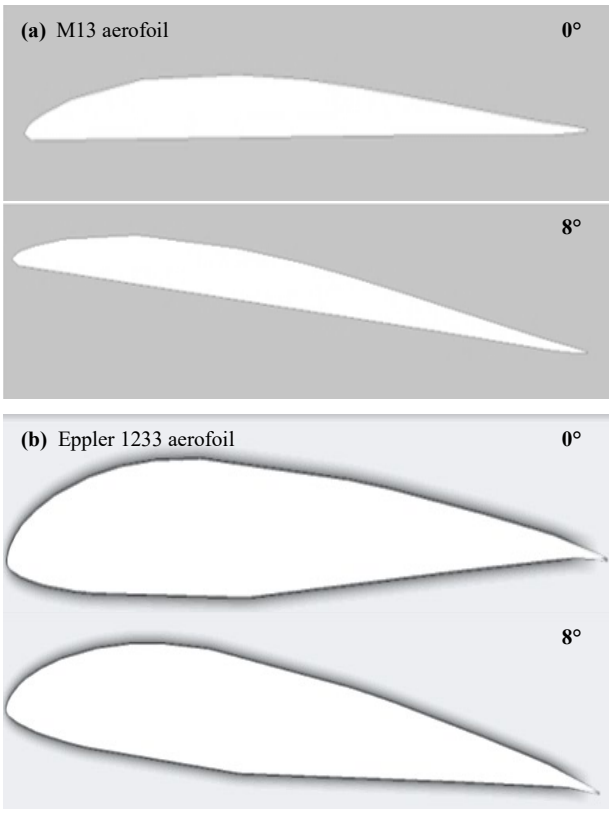

Figure 1. Different structures of the aerofoil.

The present study used four different element sizes to constantly re-mesh the airfoil. The numerical force value reaches a stable state when the number of components reaches one million, as seen. In this study, a mesh element size of 4.13 lakhs has been selected for the remaining analysis. This choice was made after considering the suitable amount of elements and a relative inaccuracy of 3%, which is considered acceptable and allows for a quicker resolution. Figure 2 depicts the different components of the air foil structure, as well as the forces exerted on them, at varying dimensions.

After completing the mesh design, it is crucial to assign the limitations as an essential step. The transition between these limits is indicated by their respective entry and exit designations. The majority of effort is focused on the region around the airfoil, therefore referred to as the "airfoil wall." Figure 3 represents the meshing in and around the aerofoil structures.

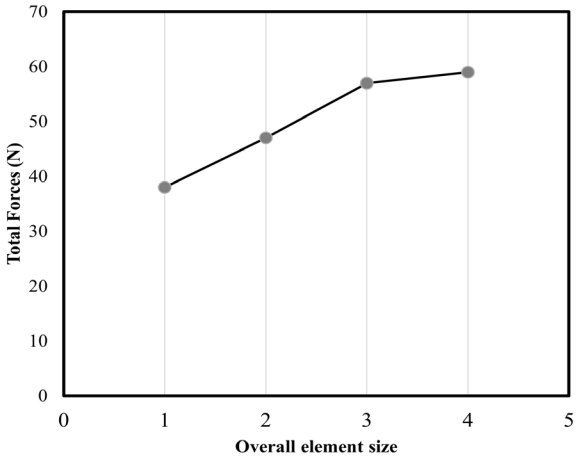

Figure 2. Grid independence study.

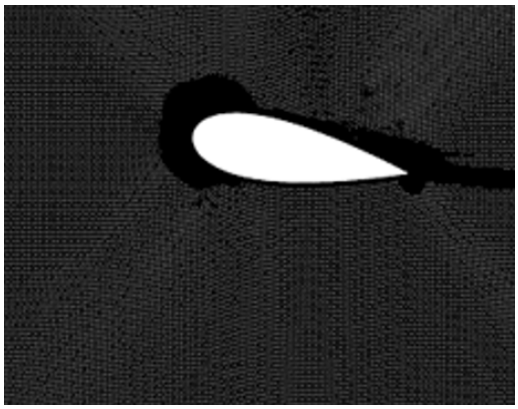

Figure 3. Meshing of the aerofoil.

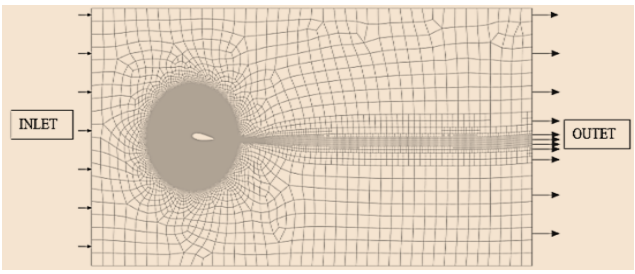

Figure 4. Inlet and outlet conditions of the flow.

In order to maintain precision in computational fluid dynamics (CFD) simulations, it is crucial to evaluate the influence of changes in mesh size on the ultimate outcomes. Augmenting the quantity of nodes might enhance the precision of the numerical solution, although it concurrently amplifies the want for storage capacity and processing duration. The study is conducted with air serving as the fluid medium and a constant input velocity of 45 $m \cdot s^{-1}$. The inlet is located on the left surface, whereas the discharge is designated on the right surface. The outlet condition denotes the pressure at which the air departs, whereas the inlet condition pertains to the air velocity at which the air supply is introduced. The entrance and outflow boundary conditions of the air foil structure are depicted in Figure 4.

Flow analysis involves the implementation of different k-epsilon and k-omega models. The k-omega viscous model is the most suitable option for achieving accurate modeling of flow over objects. Therefore, in order to meet the convergence conditions of 10^{-5} and ensure accurate calculations of pressure, moment, and velocity, it is necessary for the problem to converge. The convergence threshold between iterations is determined by using mean error residuals.The pressure-based 2D solver in FLUENT is often used to process input data, disregarding the effects of gravity.

3. Result and discussion

A computational fluid dynamics (CFD) analysis is conducted on M13, and Eppler 1233 profiles utilizing ANSYS Fluent in this study. To begin, analyze the two-dimensional profiles of the subject. As part of the investigation, the airfoil is put to the test at two distinct angles of attack—0° and 8°, so that the most efficient design can be ascertained. The subsequent section delves into the contour and vector representations of the air flow's density, pressure, temperature, and velocity variables for every profile and angle in great detail. Figure 5 represents the results exposure 2D model.

Pressure contour over the aerofoil

Figure 6 illustrates the changes in pressure for various airfoil configurations and angles of attack. When the angle of attack is set to 0°, the airflow across all three airfoils will exhibit a very symmetrical

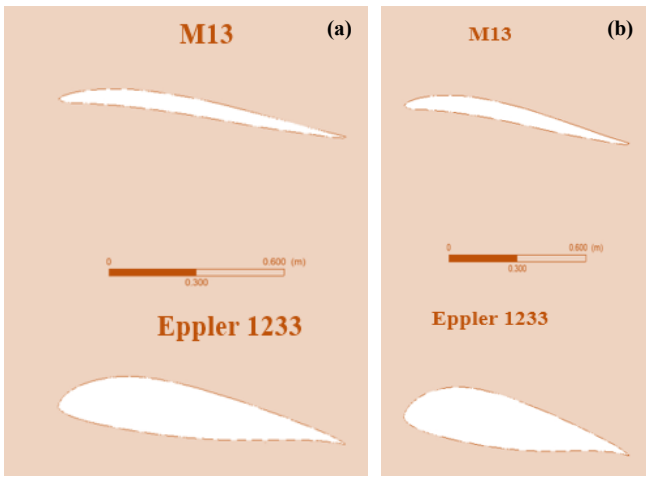

Figure 5. Flow over air foil at different structure and angle of attack, (a) 0°, and (b) 8°.

and uniform pattern, characterized by low pressure on the top surface and high pressure on the bottom surface. However, when the angle of attack rises, areas of detached and turbulent airflow will emerge, adding extra complexity to the flow. Similar to the preceding instance, the M13 airfoil will demonstrate a pressure distribution, albeit with a more conspicuous area of reduced pressure along its leading edge. More asymmetry characterizes the pressure distribution of the Eppler 1233 airfoil, which consists of a greater low-pressure region at the leading edge and a reduced high-pressure region near the trailing edge.

The pressure distribution of the Eppler 1233 airfoil will be very asymmetric due to a much larger low-pressure zone at the front edge and a minimal high-pressure region near the back edge.

3.1 Density contour over the aerofoil

When the angle of attack is zero degrees, the two airfoils' density fluctuations will be rather consistent, with only small differences due to the distribution of pressure. An increase in the angle of attack will make the disparity in density between the portions at the leading and trailing edges more apparent. Density fluctuations will also be present in the M13 airfoil, although the low-density area next to the leading edge will stand out more. With a bigger low-density zone at the leading edge and a smaller high-density portion near the following edge, the Eppler 1233 airfoil is anticipated to exhibit a more asymmetrical shift in density. Figure 6 expalins the distribution of density over the aerofoil at two different angles of attack. When the angle of attack is set to 16 degrees, the density fluctuation across the three airfoils will significantly change, ranging from 0° to 8°. The classic NACA 00224 airfoil has an uneven density distribution, characterized by a greater low-density region near the leading edge and a smaller high-density region near the trailing edge. Similarly, the M13 airfoil will have variations in density, characterized by a more prominent area of low density toward the front edge. The Eppler 1233 airfoil has a significant disparity in density distribution, characterized by a substantial low-density region at the leading edge and a comparatively modest high-density region at the following edge.

3.2 Temperature contour over the aerofoil

When evaluating aerodynamic efficiency, temperature variations that occur as airflow passes through aerofoils at various angles of attack must be taken into account. Temperature variations will be observed in the M13 aerofoil, with a region of considerably elevated temperature situated at the leading edge. A greater temperature disparity will result from the Eppler 1233 aerofoil's larger high-temperature region at the leading edge and its smaller low-temperature region near the trailing edge. The temperature distribution across the aerofoil is illustrated in Figure 7.

The M13 aerofoil, in which case the hot spot close to the leading edge is more noticeable. The Eppler 1233 airfoil's temperature variation is very asymmetrical, with a huge hot spot close to the leading edge and a little cold spot close to the trailing edge.

3.3 Velocity contour over the aerofoil

Among the most important factors affecting the aerofoil's lift and drag is the variation in flow velocity over them at different angles of attack. Figure 8 shows how different aerofoil structures and angles of attack affect velocity.

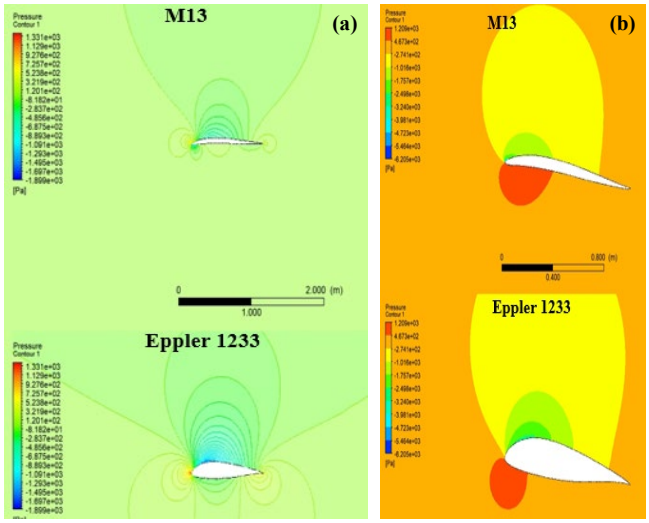

Figure 6. Pressure distribution around the aerofoil structure, (a) 0°, and (b) 8°.

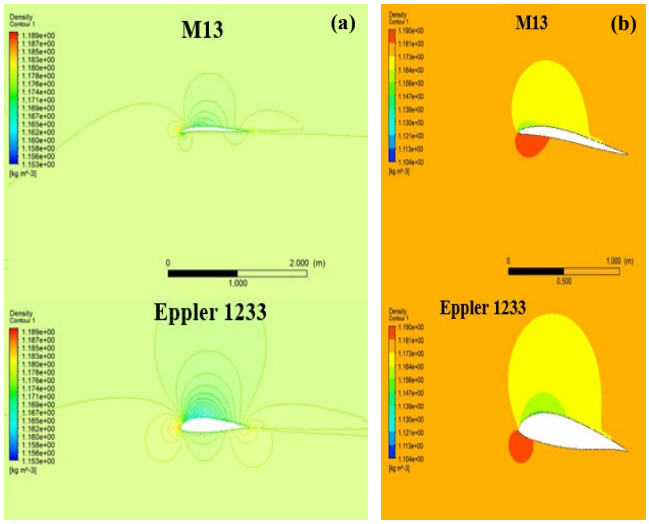

Figure 7. Density distribution around the aerofoil structure, (a) 0°, and (b) 8°.

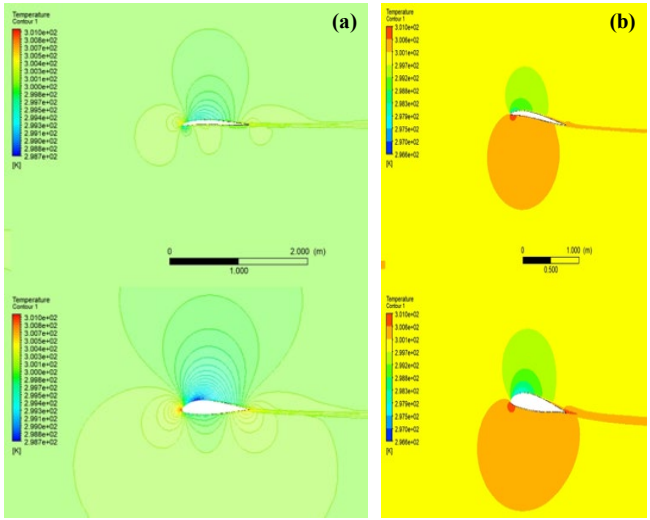

Figure 8. Temperature distribution around the aerofoil structure, (a) 0°, and (b) 8°.

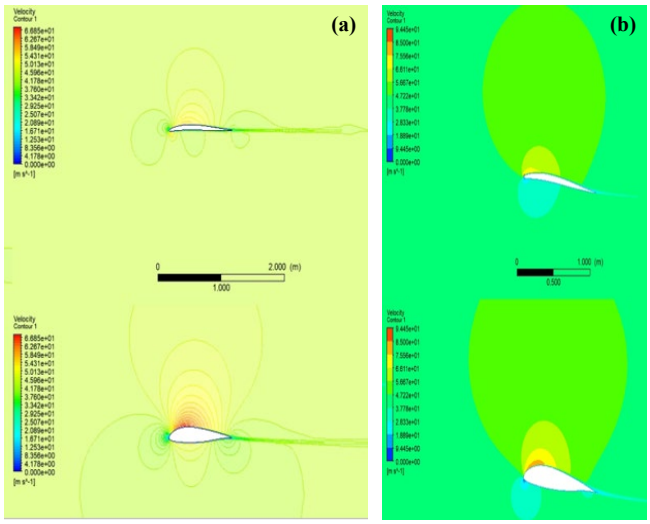

Figure 9. Velocity distribution around the aerofoil structure, (a) 0°, and (b) 8°

The M13 aerofoil, however the leading edge's high-velocity zone will be more noticeable. The Eppler 1233 aerofoil will exhibit a highly asymmetrical velocity fluctuation, with a large high-velocity zone on the leading edge and a tiny low-velocity region on the trailing edge.

As the angle of attack increases, the magnitude of the resulting drag force also increases. The resistance of the aerofoil to forward motion increases with the turbulentness of the ambient airflow at greater angles of attack. The precise correlation between drag force and angle of attack is determined by a multiplicity of factors, including the Reynolds and Mach numbers of the airflow and the characteristic shape of the aerofoil in question. In the ideal scenario, an airfoil would have a lift force that was powerful enough to do its job and a drag force that was very little. Because it affects the aforementioned parameters—altitude, speed, and weight support capacity—the lift force is a crucial design issue for airfoils. Aerofoil designers optimize the aircraft's form and size, include high-lift features like slats and flaps, and construct aerofoil shapes that encourage laminar airflow across the surface in order to improve lift force.

4. Conclusion

Evaluate and contrasted three distinct air foil and angle of attack models using ANSYS.The intake flow speed is set at 45 $m \cdot s^{-1}$ for all situations. We have investigated and compared the pressure, density, velocity, and temperature aerodynamic characteristics at various aerofoil structures and angles of attack. There is also a comparison of all aerodynamic properties using the contour photos as evidence in various scenarios.

- If the pressure on each surface stays constant at 120 Pa, the flow across all three aerofoils will be highly balanced and steady at a zero-degree angle of attack. A small amount of lift force is generated under these conditions.
- Raising the angle causes a significant build-up of pressure on the bottom of the air foil, measuring 120.7 Pa. The top side pressure at the very bottom is an indication of bad situations.
- With the exception of small differences due to pressure distribution, the two aerofoils' density fluctuations at zero degrees of attack will be almost equal. Sections with low density at the leading edge and sections with high density near the following edge will become more apparent as the angle of attack rises, with a density fluctuation of 1.153 $kg \cdot m^{-3}$ to 1.189 $kg \cdot m^{-3}$.
- It is essential to optimize the size and shape of the airfoil in order to maximize the lift force. The purpose of an airfoil's shape is to generate lift force by creating a pressure gradient between the upper and lower surfaces.
- Because the M13 achieves the most lift and has the largest pressure differential over its blade surface, it is the ideal airfoil to use in most situations.

References

[1] N. Ahmed, B. S. Yilbas, M. O. Budair, "Computational study into the flow field developed around a cascade of NACA 0012 airfoils," *Computational Methods Application Mechanical Engineering*, vol. 167, pp. 17-32, 1998.

[2] M. Arvind, "CFD analysis of static pressure and dynamic pressure for naca 4412," *International Journal of Engineering Trends and Technology*, vol. 4, pp. 3258-3265, 2010.

[3] P. Bernett, "Effect of winglets induced tip vortex structure on the performance of subsonic wings," *Aerospace Science and Technology*, vol. 10, pp. 328-340, 2016.

[4] F. M. Catalano, and H. D. Ceron-Munoz, "Experimental analysis of aerodynamics characteristics of adaptive multi-winglets," *43rd AIAA Aerospace Sciences Meeting*, vol. 10, p. 1231, 2005.

[5] B. C. Mathew, A. Thakan, M. L. Jeyan, "A review on aero-dynamic performance of NACA air foil for various Reynolds number," *International Conference on Thermo-fluids and Energy Systems,* vol. 2, p. 012003, 2018.

[6] C. K. Chen, and C.H. Hsiun, "Aerodynamic characteristics of a two dimensional air foil with ground effect," *Journal of Aircraft,* vol. 33, pp. 386-392, 1996.

[7] J. M. Kuhlman, and P. Liaw, "Winglets on low-aspect-ratio wings," *Journal of Aircraft* 25, vol. 10, pp 932- 941, 2019.

[8] D. W. Dawson, "A practical computer method for solving ship-wave problems," in *Proceedings of the second international conference on numerical ship hydrodynamics. USA*, 1977.

[9] E. Douvi, T. I. Athanasios, D. P. Margaris, "Evaluation of the turbulence models for the simulation of the flow over a National Advisory Committee for Aeronautics (NACA) 0012 airfoil," *Journal of Mechanical Engineering Research*, vol. 4, pp. 100-111, 2012.

[10] S. Goel, "Turbine air foil optimization using Quasi-3D analysis codes," *International Journal of Aerospace Engineering*, vol. 2, p. 16875974, 2008.

[11] I. Sadaq , S. N. Mehdi, S. D. Mehdi, and S. Yasear. "Analysis of NACA 0020 aerofoil profile rotor blade using CFD approach," *Materials Today: Proceedings*, vol. 64, pp. 147-160, 2022.

[12] R. Kavya, "Multi-winglets: Multi-objective optimization of aerodynamic shapes," *11th World Congress of Computational Mechanics*, vol. 56, pp. 87-112, 2019.

[13] P. J. Kunz, and I. Kroo, "Analysis, design and testing of airfoils for use at ultra-low reynolds numbers, proceedings of the

conference on fised, flapping and rotary vehicles at very low reynolds numbers," *edited by T. J. Mueller, Univ. of Notre Dame, Notre Dame, IN*, pp.349-372, 2000.

[14] E. Livne, and T. A. Weisshaar, "Aeroelasticity of nonconventional airplane configurations-past and future," *Journal of Aircraft*, vol. 40, pp. 1047-1065, 2003.

[15] M. Avvad, Vishwanath, A. R. Kaladgi, R. Muneer, M. Kareemullah, I. M. Navaneeth, "Performance analysis of aerofoil blades at different pitch angles and wind speeds," *Materials Today: Proceedings*, vol. 47, pp. 6249-6256, 2021.

[16] N. Haquea, M. Alia, and I. Ara, "Experimental investigation on the performance of NACA 4412 aerofoil with curved leading edge planform," *Procedia Engineering*, vol. 105, pp. 232- 240, 2015.

[17] A. O. Nuhait, and M. F. Zedan, "Numerical simulation of unsteady flow induced by a flat plate moving near ground," *Journal of Aircraft*, vol. 30, pp. 611-617, 1993.

[18] D. Steinbach, "Comment on aerodynamic characteristics of a two dimensional air foil with ground effect," *Journal of Aircraft,* vol. 34, pp. 445-456, 1997.

[19] T. Sumaryada, A. M. Jaya, and A. Kartono, "Simulating the aerodynamics profiles of NACA 4312 air foil in various incoming airspeed and gurney flap angle," *Journal of Physics and Physics Education,* vol. 4, pp. 1-6, 2018.

[20] S. R. Yuvaraj, and P. Subramanyam, P. "Design and analysis of wing of an ultralight aircraft," *International Journal of Innovative Research in Science, Engineering and Technology*, vol. 4, pp. 7456-68, 2015.

[21] B. Gugulothu, P. S. Satheesh Kumar, B. Srinivas, A. Ramakrishna, and S. Vijayakumar, "Investigating the material removal rate parameters in ECM for Al 5086 alloy-reinforced silicon carbide/ flyash hybrid composites by using Minitab-18," *Advances in Materials Science and Engineering*, vol. 2021, no. 1, pp. 1-6, 2021

[22] S. Vijayakumar, N. Dhasarathan, P. Devabalan, and C. Jehan, "Advancement and design of robotic manipulator control structures on cyber physical production system," *Journal of Computational and Theoretical Nanoscience*, vol. 16, no. 2, pp. 659-663, 2019.

[23] M. Rajesh, M. N. S. Sri, S. Jeyakrishnan, P. Anusha, J. E. Manikanta, N. Sateesh, B. Ch. Nookaraju, R. Subbiah, and S. Vijayakumar, "Optimization parameters for electro discharge machining on Nimonic 80A alloy using grey relational analysis," *International Journal on Interactive Design and Manufacturing (IJIDeM)*, vol. 18, pp. 1429-1442, 2024.

[24] B. Gugulothu, K. Bharadwaja, S. Vijayakumar, T. V. J. Rao, M. N. S. Sri, P. Anusha, and M. K. Agrawal, "Modeling and parametric optimization of electrical discharge machining on casted composite using central composite design," *International Journal on Interactive Design and Manufacturing (IJIDeM)*, vol. 18, no. 5, pp. 1-11, 2023.

[25] P. Sharma, P. Paramasivam, B. J. Bora, and V. Sivasundar, "Application of nanomaterials for emission reduction from diesel engines powered with waste cooking oil biodiesel," *International Journal of Low-Carbon Technologies*, vol. 18, pp. 795-801, 2023.